International Journal of Pharmaceutics 659 (2024) 124232

Contents lists available at ScienceDirect

International Journal of Pharmaceutics

journal homepage: www.elsevier.com/locate/ijpharm

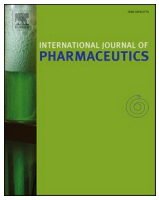

A modified Kushner-Moore approach to characterising small-scale blender performance impact on tablet compaction

Hikaru G. Jolliffe [a], Martin Prostredny [a], Carlota Mendez Torrecillas [a], Ecaterina Bordos [a], Collette Tierney [a], Ebenezer Ojo [a], Richard Elkes [b], Gavin Reynolds [c], Yunfei Li Song [b], Bernhard Meir [d], Sara Fathollahi [e], John Robertson [a,*]

[a] CMAC, Technology and Innovation Centre, 99 George Street, Glasgow G1 1RD, UK
[b] GSK Ware R&D, Harris's Lane, Ware, Hertfordshire SG12 0GX, UK
[c] Oral Product Development, PT&D, Operations, AstraZeneca UK Limited, Charter Way, Macclesfield SK10 2NA, UK
[d] Gericke AG, Althardstrasse 120, CH-8105 Regensdorf, Switzerland
[e] DFE Pharma GmbH & Co. KG, Kleverstrasse 187, 47568 Goch, Germany

ARTICLE INFO

Keywords:
Continuous direct compaction
Powder blending
Formulation
Tablets
Models
Predictions
Tensile strength
MMIC

ABSTRACT

Continuous Direct Compaction (CDC) has emerged as a promising route towards producing solid dosage forms while reducing material, development time and energy consumption. Understanding the response of powder processing unit operations, especially blenders, is crucial. There is a substantial body of work around how lubrication via batch blender operation affects tablet critical quality attributes such as hardness and tensile strength. But, aside from being batch operations, the design of these blenders is such that they operate with low-shear, low-intensity mixing at Froude number values significantly below 0.4 (Froude number *Fr* being the dimensionless ratio of inertial to gravitational forces). The present work explores the performance of a mini-blender which has a fundamentally different mode of operation (static vessel with rotating blades around a mixing shaft as opposed to rotating vessel with no mixing shaft). This difference allows a substantially wider operating range in terms of speed and shear (and *Fr* values). The present work evaluates how its performance compares to other blenders studied in the literature. Tablet compaction data from blends produced at various intensities and regimes of mixing in the mini-blender follow a common trajectory. Model equations from literature are suitably modified by inclusion of the Froude number *Fr*, but only for situations where the Froude number was sufficiently high ($1 < Fr$). The results suggest that although a similar lubrication extent plateau is eventually reached it is the intensity of mixing (*i.e.* captured using the Froude number as a surrogate) which is important for the lubrication dynamics in the mini-blender, next to the number of revolutions. The degree of fill or headspace, on the other hand, is only crucial to the performance of common batch blenders. Testing using alternative formulations shows the same common trend across mixing intensities, suggesting the validity of the approach to capture lubrication dynamics for this system.

1. Introduction

Faced with high R&D costs and an environment where efficiency in terms of both development time and material is increasingly critical, the pharmaceutical industry is exploring novel approaches to manufacturing and research (DiMasi et al., 2016). One paradigm shift that is gaining traction is continuous manufacturing of pharmaceuticals (Lee et al., 2015). Long the norm in other industries such as Oil & Gas, the potential benefits of continuous manufacturing are more economical operation, increased efficiency, and improved quality and safety (Dallinger and Kappe, 2017; Gutmann and Kappe, 2015; Plumb, 2005; Schaber et al., 2011; Yoshida et al., 2011).

Continuous Direct Compaction (CDC) of solid dosage forms is receiving significant attention both in research and industrial production, with one of the key benefits being the simplicity of manufacturing route and reduction in scale up; a variety of manufacturers have introduced continuous systems for drug product production in recent years (Fette, n.d.; GEA, 2016; Gericke, 2023; Glatt, 2023; Hosokawa Micron, n.d.; Lödige, 2023). Blending of the powder becomes key, both at the

* Corresponding author.
E-mail address: j.robertson@strath.ac.uk (J. Robertson).

https://doi.org/10.1016/j.ijpharm.2024.124232
Received 30 January 2024; Received in revised form 2 May 2024; Accepted 14 May 2024
Available online 16 May 2024

Nomenclature

Symbol	Definition and units
H	Headspace fraction (-)
Fr	Froude number (-)
F_{tablet}	Tablet breaking force (hardness) (N)
g	Gravitational constant (m•s^{-2})
K	Process-dependent variable in Eq. (1) (dm)
k_b	Bonding capacity (-)
L	Mixing length scale (dm)
n	Exponent in Eqs. (12) and (13) (-)
R	Number of revolutions (-)
r	Mixing (blade tip) radius (m)
t	Time (s)
V	Volume (L)
β	Parameter in Eq. (4) (-)
γ	Lubrication extent sensitivity to mixing parameter (dm^{-1})
ε	Porosity (-)
ν	Rotation rate (RPM)
σ	Tensile strength (MPa)
σ_0	Tensile strength at zero porosity (MPa)
$\sigma_{SF=X}$	Tensile strength at solid fraction X (MPa)
$\sigma_{SF=X,max}$	Maximum tensile strength at solid fraction X (MPa)
$\sigma_{SF=X,min}$	Minimum tensile strength at solid fraction X (MPa)
ω	Angular frequency (rad•s^{-1})

macromixing and micromixing scales (García-Muñoz et al., 2018; Karttunen et al., 2020; Moghtadernejad et al., 2018). The latter in particular benefits from rapid, high-shear mixing (Palmer et al., 2020). In a continuous blender, however, there can be a trade-off: increased RPMs may promote better micromixing, but at the cost of reduced residence time which may lead to incomplete mixing and poor content uniformity (Galbraith et al., 2020). This has led to interest in semi-continuous mini-blend systems which allow decoupling of RTD and shear input but requires an appropriately designed downstream line (Jaspers et al., 2023). Furthermore, in early stages of pharmaceutical development there may not be enough material to adequately characterise continuous blenders which typically have large mass holdup capacities, leading to difficulties in completely characterising CDC process lines. The use of smaller, semi-continuous repeat mini-blender systems as a modular stand-in for fully-continuous devices can potentially fill the gap during early stages of process development while providing approximations of the integrated CDC process benefits (Janssen et al., 2023).

Suitable mixing of powder is relevant not just for content uniformity of the Active Pharmaceutical Ingredient (API), but also for other Critical Quality Attributes (CQA) of the final product *i.e.* the solid tablet. Lubricants, such as magnesium stearate (MgSt), are added to formulations to aid the compaction process. After compression in dies, tablets must be ejected. However, without sufficient lubrication, significant force may be required to do so, and material can also stick to die walls and punch faces, leading to tablet defects and poor tablet appearance. However, excessive lubrication can negatively impact tablet hardness (Kushner and Moore, 2010), and tablets must be hard enough to survive transport, packaging and handling (but not so durable as to negatively impact disintegration and dissolution). Understanding how blenders affect the lubrication extent via mixing intensity and duration is an ongoing field of study.

In the literature, there have been various works exploring models for the scale-up of batch blending operations and the impact that lubrication extent has on tablet tensile strength (Kushner, 2012; Kushner and Moore, 2010; Kushner and Schlack, 2014). Applicable to Turbula, V-blenders, and bin blenders, the following equation was developed for tablet tensile strength at 0.85 solid fraction:

$$\sigma_{SF=0.85} = \sigma_{SF=0.85,min} + \left(\sigma_{SF=0.85,max} - \sigma_{SF=0.85,min}\right)e^{-\gamma K} \quad (1)$$

where $\sigma_{SF=0.85,min}$ is lowest possible tensile strength that can be achieved through blending, $\sigma_{SF=0.85,max}$ is the theoretical tensile strength of an unblended mixture, γ is a rate constant, and K is a measure of lubrication extent. The first three are formulation-dependant fitting parameters, and K is a process-dependent variable that has been expressed in the literature as follows:

$$K = LHR \quad (2)$$

where L is the mixing characteristic length scale, H is headspace fraction (inverse of degree of fill; bulk density is assumed), and R is the number of revolutions of the batch blender experienced by the material. The variable L depends on what type of batch blender is being used, and for bin, V and Turbula blenders is a function of volume V ($V^{1/3}$ for bin and V-blenders, 1.5 $V^{1/3}$ for Turbula blenders due to dual axis of rotation) (Kushner and Schlack, 2014). The number of revolutions R is calculated form blending time t (s) and rotation rate ν (RPM):

$$R = \frac{t\nu}{60} \quad (3)$$

The following expression can also be used instead of Eq. (1):

$$\sigma_{SF=0.85} = \sigma_{SF=0.85,max}\left(1 - \beta + \beta e^{-\gamma K}\right) \quad (4)$$

$$\beta = \frac{\sigma_{SF=0.85,max} - \sigma_{SF=0.85,min}}{\sigma_{SF=0.85,max}} \quad (5)$$

The approach outlined in Eqs. (1)–(5) have been shown valid for low-shear batch blenders from the lab scale (Kushner, 2012; Kushner and Moore, 2010) to commercial scale (Kushner and Schlack, 2014). The approach is also applicable up to the 0.4 Froude number (Fr) range, where Fr is defined as the ratio of centrifugal forces to the downward acceleration from gravity:

$$Fr = \frac{\omega^2 r}{g} \quad (6)$$

where ω is angular frequency, r is the radius of the mixer, and g is the gravitational constant. Powder mixing inside a closed vessel is said to have the following flow regimes: tumbling ($Fr < 0.4$, also referred to as simple stirring), transitional or partial inertial ($0.4 < Fr < 2$) or centrifugal ($2 < Fr$) (Brone et al., 1998).

As rotation rate (and angular frequency) increases, the centrifugal forces begin to dominate. For batch blenders that operate by moving the entire vessel (bin blenders, V-blenders, Turbula blenders) this inhibits mixing as material is forced to the vessel walls and can no longer move freely; the variable H in Eq. (2) has a similar function – if a blender is completely full (*i.e.* $H = 0$) then the powder can no longer move and mixing cannot occur. Typical operating conditions for batch blenders have Fr significantly below 0.4 (Brone et al., 1998).

A mini blender is less restricted than the $Fr < 0.4$ regime, as it operates by rotating blades about a mixing shaft, and powder will still move when higher centrifugal forces are present ($Fr \gg 1$; Fig. 1, Fig. 2). With a mini-blender, even with $Fr > 1$ there is a substantial amount of material as a tumbling powder bed in the lower part of blender (likely as the blades cannot act on every part of the mixture at once), and it is only at extremely high RPM (and Fr) that material moves in a near continuous annulus near the vessel walls. It has been reported in the literature that three mixing regimes can be defined for the mini-blender: push mixing

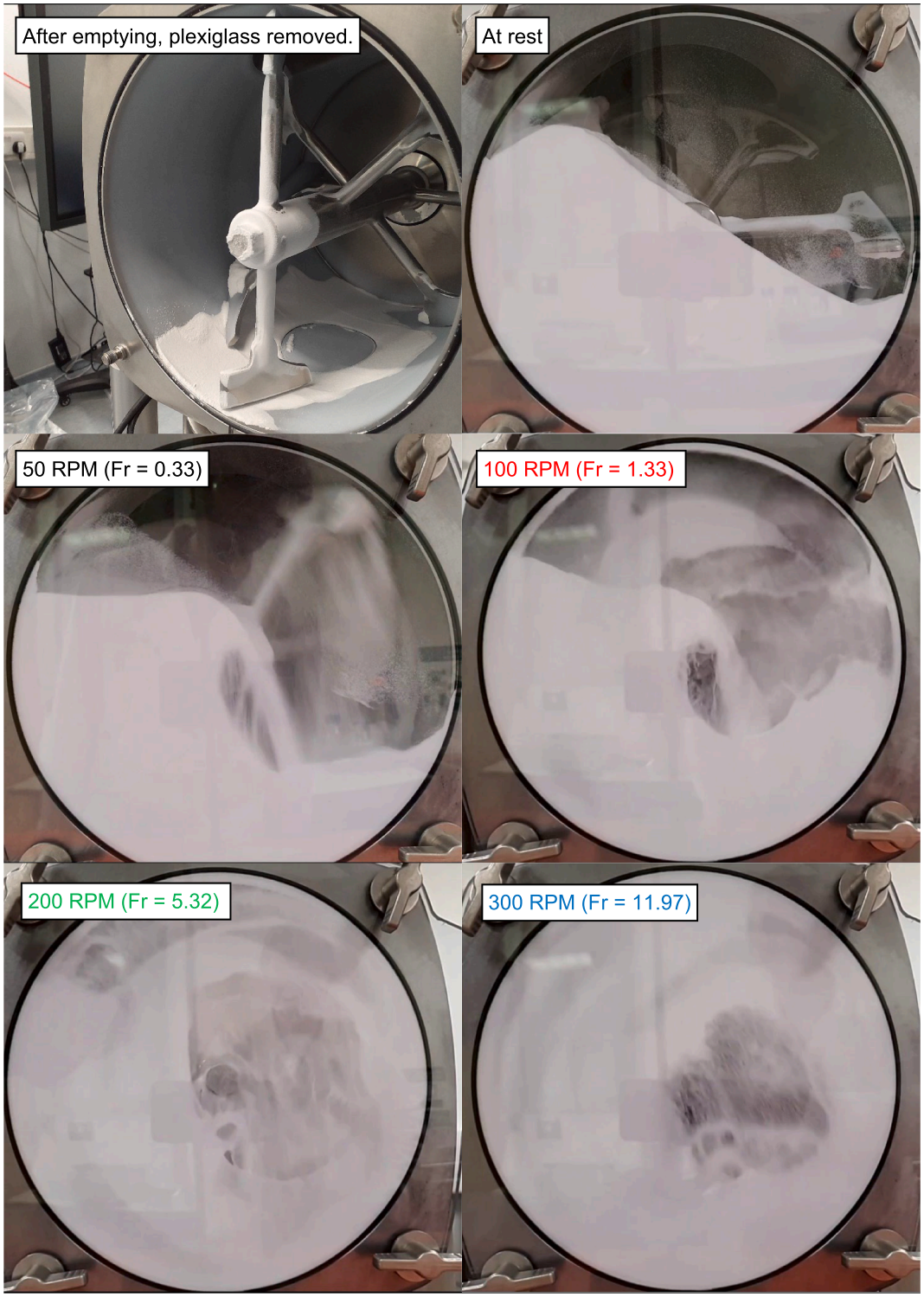

Fig. 1. Detail of the Gericke GBM 10P Mini Blender, with a spray-dried lactose product (Fast Flo® 316) at 50 % fill level. Images extracted from high-speed video.

($Fr < 2.5$), spin mixing ($2.5 < Fr < 11$), and centrifugal mixing ($11 < Fr$) (Jaspers et al., 2023).

As stated previously, the semi continuous mini-blend allows decoupling of shear rate and residence time and allows access to a variety of flow regimes leading to the potential for a wide range of mixing intensities and hence lubrication extents to be generated. The objective of the present work is to explore how operating conditions impact the lubrication extent of a mini-blend system and to see how applicable the approach of Eq. (1) (developed on blenders that are rotating vessels with no blades and low *Fr* values) scales to the mini-blender (static vessel with rotating blades at operable at both low and high RPM equating to low and high *Fr*) and if it needs to be modified in any way. If applicable, the objective is to then assess how the resulting approach could be scaled or otherwise translated to allow observed behaviour in a mini blender to be scaled to predict performance in a tumble batch blender (or vice versa). This would inform scaling of lubrication extent between typical batch tumble blend processes and tested mini-blend process.

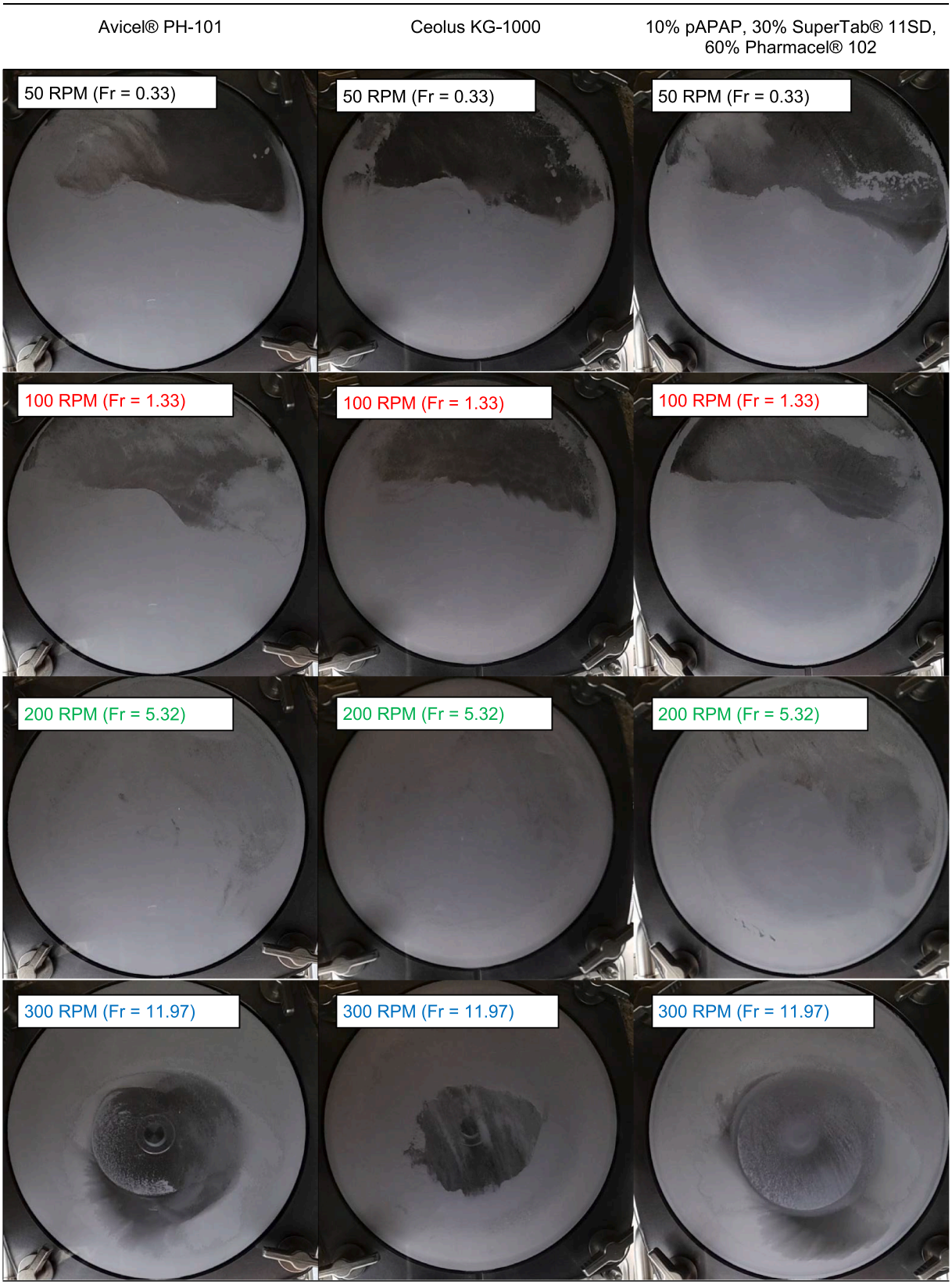

Fig. 2. Detail of the Gericke GBM 10P Mini Blender at 50 % fill and various RPMs. Contents are Avicel® PH-101, Ceolus KG-1000 and a formulation of 10 % powdered paracetamol (Mallinckrodt), 30 % SuperTab® 11SD, 60 % Pharmacel® 102. Images extracted from high-speed video.

2. Materials and methods

2.1. Design of experiments

The intent of the present work is to build on and expand prior efforts by various research groups (Kushner, 2012; Kushner and Moore, 2010; Kushner and Schlack, 2014). An initial set of scoping runs (Table 2, runs 6–10; runs have been re-numbered to make tables easier to follow) explored a range of blending speeds (100, 200, 300 RPM) and blending times (5 s, 10 s, 30 s, 60 s, 120 s, 600 s, 1200 s) to cover a comparable x-axis range (7–2605 dm) as the prior work (approx. 0–4000 dm).

During analysis, it was found that adjusting the literature approach by modifying the x-axis by inclusion of the Froude number may be beneficial in identifying one overall trend for all blender speeds and fill levels. When data are plotted in this manner, there are some gaps along the new x-axis that subsequent runs have been chosen to fill, and these include those at a lower speed of 50 RPM (Table 2, runs 1–5), and alternative degrees of fill (Table 2, runs 25–30), and additional blending times to expand the initial scoping datasets of 100, 200, and 300 RPM (Table 2, remaining runs up to 24).

Additionally, the approach was tested using an alternative formulation, and select run conditions at the standard 3 kg fill level (Table 2, runs 25–38).

2.2. Materials and equipment

To visualise flow regimes at different blender speeds (Fig. 1, Fig. 2); Fast Flo® 316 (Kerry), Ceolus KG-1000 (Asahi Kasei); Avicel® PH-101 (Dupont); and a blend of powdered paracetamol (Mallinckrodt), SuperTab® 11SD (DFE) and Pharmacel® 102 (DFE) have been used. For blending experiments, the materials used were selected based on previous work in the literature to allow a comparison of trends (Kushner and Moore, 2010). The formulation composition is based on a 2:1 ratio of microcrystalline cellulose (MCC; Pharmacel® 102, DFE) to lactose monohydrate (SuperTab® 11SD, DFE) adding up to 99 % of the blend and 1 wt% of magnesium stearate (Ligamed® MF-2 V, Peter Greven). The composition is fixed to allow exploration of the effect of blending conditions. In latter experiments, the MCC-lactose ratio has been flipped to test whether the observed forms of relationship hold across different blend properties. The material bulk and tapped density measurements have been carried out following the British Pharmacopeia guidelines 2023 (Appendix XVII S. Bulk Density and Tapped Density of Powders). The tapped density has been measured using a tapped density analyser (Autotap, Quantachrome, Anton Paar GmbH, Graz, Austria). True density analysis has been measured using a gas Pycnometer (MicroUltrapyc 1200e, Quantachrome, Anton Par GmbH, Graz, Austria) connected to a water bath at 25 °C. The sample weight was measured using a laboratory balance (BP211D Analytical model, Sartorious, Surrey, United Kingdom) repeated three times and averaged.

Particle size distributions (included for information only) were measured in triplicate using a Mastersizer® 3000 (Malvern Panalytical, Worcestershire, United Kingdom) fitted with a dry dispersion cell and varying the pressure between 1 and 3 to maintain a constant flow. The hopper was set at 3.0 mm height and between 500 mg and 1000 mg of sample was used. The limits for particle size analysis were chosen per ISO 3310:2016. Analysis results are given in Table 1.

The blenders used are a GBM 10P Mini Blender (Fig. 3, a horizontal single shaft mixer of 10 L from Gericke AG Switzerland; measured volume 11.59 L, blade radius 0.119 m) and a 5 L Pharmatech bin blender (with an effective mixing radius – the distance from axis of rotation to furthest point in the bin – of 0.158 m). Tablets were compacted in a KORSCH XP 1 single-punch tablet press.

2.3. Mini-blender operation

Blending speed and time were varied to explore a range of degrees of mixing (time from 5–3000 s, blending speed from 50 to 300 RPM) covering all potential regimes of mixing (Jaspers et al., 2023). The blender typically held 3 kg of material, with select runs at 2.25 kg and 3.75 kg to explore the effect of fill level on lubrication extent.

For all experiments, a fixed routine of blend material addition was adopted with Pharmacel® 102 added first followed by SuperTab® 11SD, and pre-blended at 100 RPM for 60 s for all runs, with relative quantities as per Table 2; during blender filling (material addition), speed was set to 10 RPM for 1 s. For the lubricant addition step lubricant quantity and type, blending time and speed were varied as described in Table 2. Material was added manually. Blender discharge was set to 10 RPM for 1200 s to allow for complete discharge (200 revolutions, however the vast majority of material discharges within the first few revolutions). Discharged blend masses were recorded to allow calculation of blender heel amount. Blends were collected from the blender and stored until compaction experiments in sealed plastic bags with limited headspace to avoid any post-blending effects. These blends were then used for compaction, where a required amount of each blend was loaded into the tablet press hopper.

Each blender run is completely discharged as taking smaller, intermitted samples during one run is not practical, entailing stopping the experiment multiple times (alongside the required speeding up and slowing down of the blades) and the degree of fill would be affected. Furthermore, to fill the tablet press simulator, larger quantities of material were needed than that needed for the specific tablets used during analysis for each run.

2.4. Bin blender (BB) operation

All blends were prepared with a Pharmatech bin blender with a 5 L IBC vessel without the inner agitator at a target blend mass of 1.5 kg. A fixed pre-blend time of 10 min at 20 rpm was used for the main excipients. The same sequence of material addition was maintained with MCC (Pharmacel® 102) added first, followed by lactose (SuperTab® 11SD). For the lubricant (Ligamed® MF-2 V) addition step, a fixed speed of 20 rpm was used and blending time was varied as described in Table 3. Blends were collected from the blender and stored until compaction experiments in sealed plastic bags with limited headspace to avoid any post-blending effects. These blends were then used for compaction, where a required amount of each blend was loaded into the tablet press hopper.

Table 1
List of materials, physical properties and formulation compositions used in blending experiments. Particle size and tapped density are included for information purposes only. a: estimated.

Material	Grade / supplier	Role in blend	Weight % in formulation	Density (g/cm^3)			Particle size (μm)		
				Bulk	Tapped	True	d_{10}	d_{50}	d_{90}
Lactose monohydrate	SuperTab® 11SD / DFE	Filler	33 or 66	0.61	0.71	1.54	39.65	111.50	246.25
Microcrystalline cellulose	Pharmacel® 102 / DFE	Compression aid	66 or 33	0.36	0.49	1.54	25.90	85.90	198.00
Magnesium stearate	Ligamed® MF-2 V / Peter Greven	Lubricant	1	0.28	0.43	1.11	1.23	5.11	22.88
66 % cellulose 33 % lactose blend				0.42	0.56	1.54	–	–	–
33 % cellulose 66 % lactose blend				0.50[a]	–	1.54	–	–	–

Table 2
Mini blender run conditions. a: standard formulation (66 % Pharmacel® 102, 33 % SuperTab® 11SD, 1 % Ligamed® MF-2 V) and fill conditions. b: changing fill conditions with standard formulation. c: flipped formulation (33 % Pharmacel® 102, 66 % SuperTab® 11SD, 1 % Ligamed® MF-2 V).

Run	Blending speed **(RPM)**	Blending time **(s)**	Revolutions ***R***	Blend mass **(kg)**	Blend bulk density **(g/cm3)**	Headspace fraction ***H***	**Froude number *Fr***
1[a]	50	659	549	3	0.42	0.38	0.33
2[a]	50	1198	998	3	0.42	0.38	0.33
3[a]	50	1797	1498	3	0.42	0.38	0.33
4[a]	50	2396	1997	3	0.42	0.38	0.33
5[a]	50	2995	2496	3	0.42	0.38	0.33
6[a]	100	5	8	3	0.42	0.38	1.33
7[a]	100	10	17	3	0.42	0.38	1.33
8[a]	100	30	50	3	0.42	0.38	1.33
9[a]	100	60	100	3	0.42	0.38	1.33
10[a]	100	120	200	3	0.42	0.38	1.33
11[a]	100	600	1000	3	0.42	0.38	1.33
12[a]	100	1200	2000	3	0.42	0.38	1.33
13[a]	200	41	137	3	0.42	0.38	5.32
14[a]	200	60	200	3	0.42	0.38	5.32
15[a]	200	75	250	3	0.42	0.38	5.32
16[a]	200	112	374	3	0.42	0.38	5.32
16R[a]	200	112	374	3	0.42	0.38	5.32
17[a]	200	187	624	3	0.42	0.38	5.32
18[a]	200	600	2000	3	0.42	0.38	5.32
19[a]	300	18	92	3	0.42	0.38	11.97
20[a]	300	33	166	3	0.42	0.38	11.97
21[a]	300	50	250	3	0.42	0.38	11.97
22[a]	300	60	300	3	0.42	0.38	11.97
23[a]	300	83	416	3	0.42	0.38	11.97
24[a]	300	600	3000	3	0.42	0.38	11.97
25[b]	100	30	50	2.25	0.42	0.54	1.33
26[b]	100	30	50	3.75	0.42	0.23	1.33
27[b]	100	120	200	2.25	0.42	0.54	1.33
28[b]	100	120	200	3.75	0.42	0.23	1.33
29[b]	200	60	200	2.25	0.42	0.54	5.32
30[b]	200	60	200	3.75	0.42	0.23	5.32
31[c]	100	30	50	3	0.38	0.32	1.33
32[c]	100	165	275	3	0.38	0.32	1.33
33[c]	200	41	137	3	0.38	0.32	5.32
34[c]	300	18	90	3	0.38	0.32	11.97
35[c]	100	300	500	3	0.38	0.32	1.33
36[c]	300	33	165	3	0.38	0.32	11.97
37[c]	100	1200	2000	3	0.38	0.32	1.33
38[c]	300	133	665	3	0.38	0.32	11.97

2.5. Tableting protocol

Tableting was performed with a single station KORSCH XP1 tablet press equipped with 9 mm round flat faced punches operating at a frequency of 20 S per minute. The fill depth (lower punch position) was adjusted to ensure a tablet target weight of 200 mg for each blend. For the compression profile determination, tablets were compressed at 8 upper main compression force (UMCF) points from 1 to 36 kN. Compaction data such as upper and lower mean compression forces, as well as upper and lower punch displacement and ejection force were collected. A total of 100 tablets were prepared for each compression point. From these 10 were used for hardness/ tensile strength determination, the remaining ones were retained for further analysis. Data acquisition from the KORSCH software interface (EDA) was carried out by taking individual values for each tablet whose weight, height and hardness were analytically measured.

Tablet weight was measured with a 5DP analytical balance. Tablet height and hardness were measured using a calibrated hardness tester (Kraemer Elektronik, Germany) with 2 different load cells: 0–50 N or 50–500 N crushing force according to the expected tablet hardness.

2.6. Compaction analysis

Data for tablet tensile and porosity have been used to regress parameters of the Ryshkewitch-Duckworth equation (Duckworth, 1953; Ryshkewitch, 1953):

$$\sigma = \sigma_0 e^{-k_b \varepsilon} \tag{7}$$

where σ is tensile strength, σ_0 is tensile strength at zero porosity (a fitting parameter), k_b is the bonding capacity (a fitting parameter), and ε is porosity. The regression has been done in Matlab R2022a.

$$\sigma = \frac{2F_{tablet}}{1,000,000\pi d_{tablet} h_{tablet}} \tag{8}$$

where F_{tablet} is the measured breaking force, d_{tablet} is the diameter of the tablet (set by the die), and h_{tablet} is the tablet height (or thickness; measured).

Tablet porosities are calculated from experimental data of tablet mass, thickness, and true density:

$$\varepsilon = 1 - \frac{\rho_{tablet}}{\rho_{true}} \tag{9}$$

$$\rho_{tablet} = \frac{m_{tablet}}{V_{tablet}} \tag{10}$$

$$V_{tablet} = \pi \left(\frac{d_{tablet}}{2}\right)^2 h_{tablet} \tag{11}$$

where ρ_{tablet} is the density of the compacted tablet (calculated), ρ_{true} true density of the formulation (measured), m_{tablet} is the tablet mass (measured), V_{tablet} is the volume of the tablet (calculated).

Tablets typically have a porosity of 0.15–0.25 *i.e.* a solid fraction of 0.85–0.75 (Nassar et al., 2021). For further analysis purposes, values of tensile strength at 0.85, 0.80 and 0.75 solid fraction have been used (*i.e.* regressed curve values at 0.15, 0.20 and 0.25 porosity, Fig. 4).

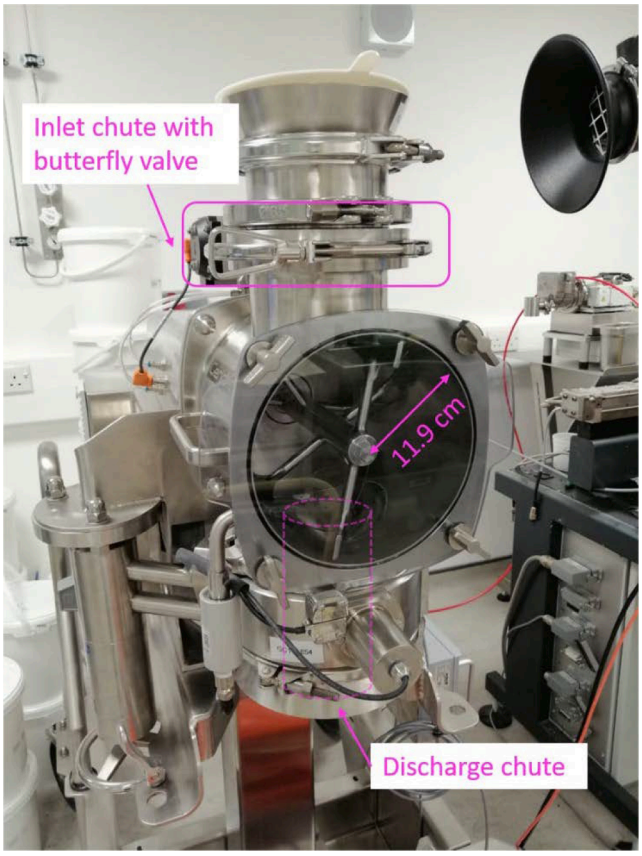

Fig. 3. The Gericke GBM 10P Mini Blender. Shown empty with Perspex window in place.

Table 3
Bin blender runs (66 % Pharmacel® 102, 33 % SuperTab® 11SD, 1 % Ligamed® MF-2 V).

Run	Blending time (s)	Blending speed (RPM)	Blend mass (kg)
BB-1	180	20	1.5
BB-2	300	20	1.5
BB-3	1800	20	1.5
BB-4	3600	20	1.5
BB-5	8400	20	1.5
BB-6	26,400	20	1.5

Experimental tensile strength values (in MPa) are calculated from tablet hardness (breaking force, in N) and thickness:

3. Results and discussion

Experiments and analysis have been conducted in stages, exploring various directions:

1. Whether, for a given formulation, tensile strength data can be plotted against a horizontal axis such that there is one overall trend, and whether there is a way to scale or translate predictions from such a 'collapsed' curve to performance in a bin blender.
2. The impact of fill level on tensile strength and collapsed curves

Compaction data for the base formulation at various blending conditions (blending time, RPM) values show that data points appear to be separate according to RPM and *Fr*, with the various sets of datapoints following what appears to be an exponential trend (Fig. 5); for a given blender design, *Fr* and RPM are correlated. Blender dimensions and RPM are the two variables that determine *Fr*. For a given x-axis value, tensile

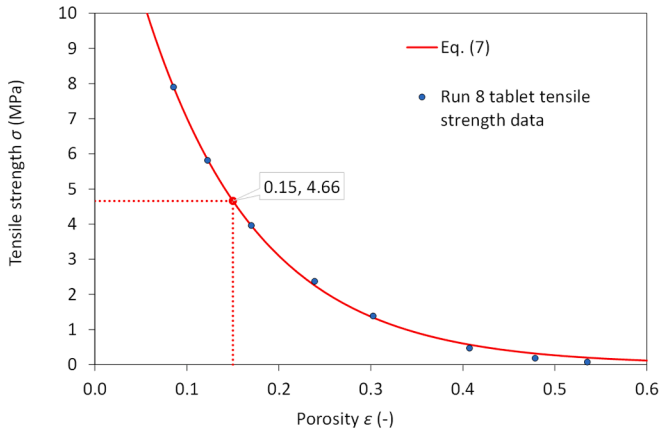

Fig. 4. Compaction data (tensile strength v porosity) for 3 kg of base formulation blended at 100 RPM for 30 s, showing interpolation to determine tensile strength at solid fraction of 0.85 (porosity of 0.15).

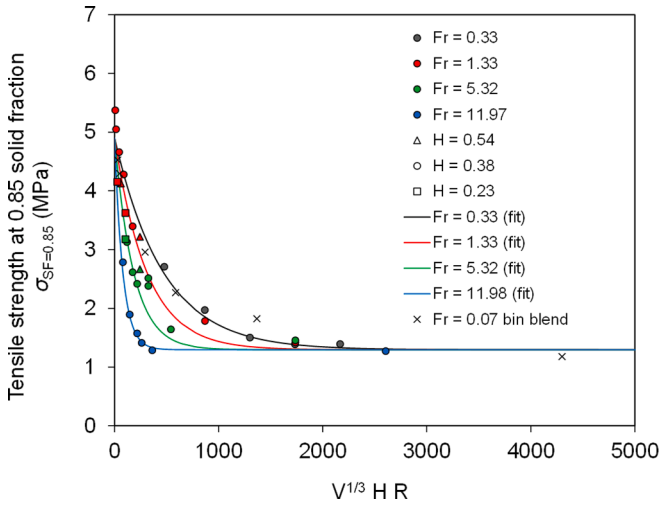

Fig. 5. Compaction data for the base formulation (Table 2, runs 1–30) plotted against the Kushner-Moore axis (Eqs. (1) and (2)). Froude numbers of 0.33, 1.33, 5.32, 11.97 correspond to 50, 100, 200 and 300 RPM, respectively. Equivalent data from material blended in a bin blender at 20 RPM (corresponding to Froude number of 0.07) is also overlaid (Table 3, runs BB-1 to BB-6). Mini blender data has contents of 2.25, 3 or 3.75 kg ($H = 0.54, 0.38, 0.23$, respectively) while the bin blender held 1.5 kg ($H = 0.28$).

strengths are lower for material blended at higher speeds. A common tensile strength plateau is reached, and in general at higher RPM, this floor is reached sooner; said otherwise, there is a lower limit to the tensile strength that can be reached for this formulation with the difference from different blender speeds being how much blending time is needed to reach a given tensile strength. This general exponential decline to a plateau behaviour is expected, and in quality is seen in other small and large tumble blenders (Kushner, 2012; Kushner and Moore, 2010; Lou et al., 2020), also evidenced by the overlaid bin blender data (Fig. 5).

With the assumption that all sets of data would share a common starting point (the formulation and blender contents mass is the same for all datapoints in Fig. 5) and that the minimum tensile strength that can be reached is also the same for the mini blender datapoints, model parameters can be regressed: $\sigma_{SF=0.85,max}$ and $\sigma_{SF=0.85,min}$ are 4.903 and 1.294 MPa, respectively (β of 0.74); and γ ranges by approximately a factor of 6 from 0.00215 to 0.01266 for mixing conducted at the various RPM values (Table 4). The parameter γ is defined and expected to be a function only of formulation components and not of process, this wide

Table 4
Regressed parameters of Eqs. (1) and (4), regressed under assumption that datasets share a common maximum and minimum ($\sigma_{SF=0.85,max}$ and $\sigma_{SF=0.85,min}$, respectively).

ν (RPM)	Fr (−)	$\sigma_{SF=0.85,max}$ (MPa)	$\sigma_{SF=0.85,min}$ (MPa)	β (−)	γ (dm^{-1})
50	0.33	4.903 ± 0.332	1.294 ± 0.176	0.74	0.00215 ± 0.00059
100	1.33	4.903 ± 0.332	1.294 ± 0.176	0.74	0.00324 ± 0.00119
200	5.32	4.903 ± 0.332	1.294 ± 0.176	0.74	0.00550 ± 0.00122
300	11.97	4.903 ± 0.332	1.294 ± 0.176	0.74	0.01266 ± 0.00364

range suggests that mini-blend process dynamics are not adequately captured using original Kushner Moore approach leading to high variability in predicted γ value. Aside from data runs conducted at different RPM values taking different trajectories (demonstrated in the different fitted values of γ), the bin blender appears to perform slightly differently, especially when the standard K axis of Eq. (2) is used. That the parameter γ has different values based on RPM suggests that the approach of Eqs. (1) and (2) is not sufficient for the mini-blender.

3.1. Collapsing lubrication extent curves

Observing the tensile strength data (Fig. 5) and visual observations (Fig. 1 and Fig. 2), it is clear that the Fr number captures the transition between flow regimes across materials and it is hypothesized Fr can thus act as a surrogate for intensity of mixing and hence lubrication extent whilst maintaining a consistent lubrication extent axis units with previous work. The only two ways to affect Fr are speed (rotation rate) and the rotational radius (with is straightforward a concept for most batch blenders). In the present work the focus is to extend mixing via the time dimension rather than size – there is access to one equipment scale for each mode of mixing (GBM 10P Mini Blender for fixed vessels with rotating blades and Pharmatech 5 L bin blender for rotating vessels with no internal blades). This implies that, for the mini-blender system in isolation, an approach that results in a uniform trend for all data points could potentially be achieved by including again the RPM in the right hand side of Eq. (2) (again as it is already used to calculate the number of rotations in R).

An iterative approach suggested that the modification of Eqs. (1) and (2) to include a Fr term with an exponent could be promising towards collapsing the various trends into one:

$$\sigma_{SF=0.85} = \sigma_{SF=0.85,min} + \left(\sigma_{SF=0.85,max} - \sigma_{SF=0.85,min}\right) e^{-\gamma V^{1/3} HR(Fr)^n} \quad (12)$$

Optimising for n in alongside the parameters of Eq. (12) returns a value of 1/2.2 for n, suggesting that the square root of Fr as a useful term to use to collapse the data (Table 5). However, as noted in the literature, there are certain mixing regimes corresponding to certain Froude numbers. The hypothesis tested is that for low Froude numbers below 1 the typical Kushner-Moore equation can be used (*i.e.* Eq. (12) with $n = 0$), but if Froude number is above 1 and the material is sufficiently agitated (Fig. 1, Fig. 2), then it is not only the number of revolutions experienced that matters, but also the intensity at which they were experienced (*i.e.* Eq. (12) with $n = ½$); this is summarised in Eq. (13):

$$\sigma_{SF=0.85} = \sigma_{SF=0.85,min} + \left(\sigma_{SF=0.85,max} - \sigma_{SF=0.85,min}\right) e^{-\gamma V^{1/3} HR(Fr)^n}, n = \begin{cases} 0 & \text{if } Fr < 1 \\ 1/2 & \text{if } Fr > 1 \end{cases} \quad (13)$$

Plotting the data in this manner results in Fig. 6. The datapoints for both the mini-blender and the bin blender now all follow a similar trajectory. The fitted parameters for the collapsed data are $\sigma_{SF=0.85,max} = 4.761$ MPa, $\sigma_{SF=0.85,min} = 1.369$ MPa, and $\gamma = 0.00272$ (Table 5, regressed to mini-blender data but not bin blender data), and are an improved fit over Eq. (12). It appears that Eq. (13) may be sufficient for the approach to be transferable between a mini-blender and other batch blenders

Table 5
Regressed parameters for data plotted for various values of n (Eq. (12), Eq. (13)).

Eq.	n	$\sigma_{SF=0.85,max}$ (MPa)	$\sigma_{SF=0.85,min}$ (MPa)	γ (dm^{-1})	RMSE
12	1	5.233 ± 1.115	1.777 ± 0.275	0.00559 ± 0.00331	1.361
12	1/2	4.874 ± 0.428	1.369 ± 0.220	0.00313 ± 0.00084	0.703
12	1/2.2	4.895 ± 0.428	1.387 ± 0.216	0.00329 ± 0.00086	0.696
12	1/3	4.953 ± 0.507	1.393 ± 0.230	0.00374 ± 0.00113	0.786
13	1/2	4.761 ± 0.395	1.369 ± 0.209	0.00272 ± 0.00071	0.685

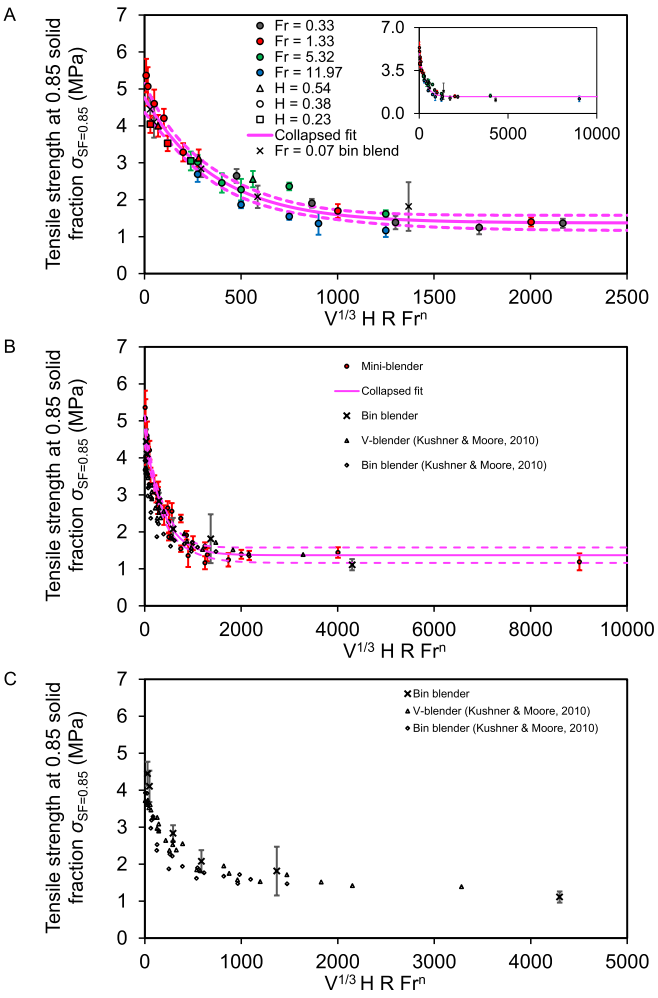

Fig. 6. Collapsed compaction data for the base formulation (Table 2, runs 1–30) plotted against the modified Kushner-Moore axis (Eq. (13)). A: Froude numbers of 0.33, 1.33, 5.32, 11.97 correspond to 50, 100, 200 and 300 RPM, respectively. Equivalent data from material blended in a bin blender at 20 RPM (Fr = 0.07, black X) also overlaid but has not been used in fitting (Table 3, runs BB-1 to BB-6). Mini blender data has contents of 2.25, 3 or 3.75 kg (H = 0.54, 0.38, 0.23, respectively) while the bin blender held 1.5 kg (H = 0.29). Curve regressed to collapsed data in magenta (with prediction intervals). B: collapsed data (red datapoints) with regressed fitted curve with prediction intervals (magenta), overlaid with literature data (Kushner and Moore, 2010). C: solely plotting bin blender and literature data. (For interpretation of the references to colour in this figure legend, the reader is referred to the web version of this article.)

(Kushner, 2012; Kushner and Moore, 2010; Kushner and Schlack, 2014), although there appears to be a slight offset between literature batch blender data and bin blender data used in the present work (Fig. 6B, Fig. 6C).

The approach appears to also hold (*i.e.* the datasets collapse onto one) for other solid fractions within a the common solid fraction target range of 0.75–0.85 with tensile strength of 1.5–2.5 MPa (Nassar et al., 2021); collapsed curves at all three solid fractions are shown in Fig. 7. When data and regressed fits within this range are focused on, the majority of datapoints fall within the criteria, and those that fall outside the criteria mostly have error bars that overlap with the accuracy thresholds (Fig. 8).

3.2. The impact of fill level on tensile strength and collapsed curves

Headspace fraction H is used in tumble blend literature account for the effect that powders in tumble blending mixing more in avalanching surface layer whose length is a function of head space. (Kushner and Moore, 2010), and so far have been retained in the present work (Eq. (13)) to more easily allow comparisons between the mini-blender and the bin blender (Fig. 6). Analysis of the data suggests however that, at least for the mini-blender, headspace fraction may not be relevant as could be expected from operating principles – repeating the analysis with H omitted from Eq. (13) (*i.e.* $H = 1$ for all datapoints, Fig. 9) results in very little difference to the regressed parameters or goodness of fit (Table 6).

Whilst it is beyond the scope of the present work to extensively explore the impact headspace fraction (degree of fill) has on lubrication extent, it could be that while mixing length scale and number of revolutions are important for both mini-blender and batch blenders such as the bin blender, for the former it is the intensity of mixing that matters (inclusion of $Fr^{1/2}$ in the model equation, assuming sufficient intensity of $1 < Fr$) whilst for the latter it is the headspace fraction that matters (aside from the fact that mixing won't occur when Fr is too high), there may be some constant value for H that applies for any condition in the mini-blender (some value is needed for transferability with bin blender or other batch blenders).

3.3. Alternative formulation

To further test whether this approach (Eq. (13)) holds when the formulation is changed, select test conditions were conducted at flipped MCC-lactose ratios (33 % Pharmacel® 102, 66 % SuperTab® 11SD; Table 2, runs 31–38). Plotting these runs alongside the base formulation (66 % Pharmacel® 102) shows that the flipped formulation (66 % SuperTab® 11SD) shows similar behaviour – with a collapsing of the curves possible – albeit at lower tensile strengths (Fig. 10). The maximum tensile strength drops from 4.761 to 3.016 MPa, while the minimum attainable tensile strength drops from 1.387 to 0.911 MPa (drops of 37 % and 33 %, respectively), and the rate constant changes from 0.00272 to 0.00324, a 20 % increase (Table 7).

That tensile strength changes as a result of change in formulation is of course to be expected – different pure components compact differently, and understanding this process (and how respective material properties affect this) is key (Martin et al., 2021; Wünsch et al., 2019). Three phenomena commonly associated with and used to describe tablet compaction are elastic (reversible), plastic (irreversible) and brittle (irreversible) deformation (Dwivedi et al., 1992; Giannis et al., 2021; Vachon and Chulia, 1999); in the first, particles change shape but largely rebound after force is removed, in the second particles do not rebound, and in the third particles break into smaller particles as a result of the compressive force.

Pharmacel® 102 is microcrystalline cellulose (MCC), a material known to be plastic which leads to significant surface area available for compaction and the formation of bonds, leading to its good performance in terms of compressibility and compactability (*i.e.* good tensile strength) (Pitt et al., 2015; Zhang et al., 2017). In contrast, SuperTab 11SD is a lactose product, and these are often known to be brittle with higher Heckel yield pressures than MCC products (and resulting in easier breakage, *i.e.* lower tensile strength) (Busignies et al., 2012, 2006; Ilić et al., 2009; Zhang et al., 2017). Whilst the tensile strength of binary tablets does not always follow a linear mixing rule (Jolliffe et al., 2019), that the MCC-heavy formulation has higher tensile strength than the lactose-heavy formulation is consistent with the known properties of those substances (Table 7).

4. Conclusions

The present work has explored modifications to established equations for how batch blender operation affects lubrication extent in tablets produced by direct compaction using a semi-continuous mini blend approach to account for the broader range of mixing intensities that can be generated in the agitated mini blend technology. Whilst the mini-blender used in the present work has a fundamentally different mode of operation than common batch blenders (bin blender, V-blender, Turbula blender), being a static cylinder with rotating blades about a shaft, results indicate that lubrication process follows similar predictable trajectory but with different process dynamics.

Tablet compaction data from blends produced at various intensities and regimes of mixing in the mini-blender follow a common trajectory

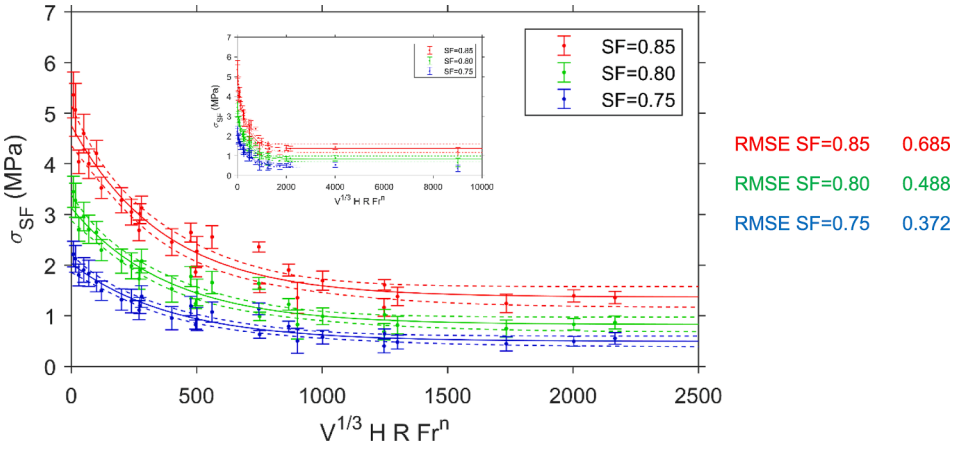

Fig. 7. Red: collapsed compaction data for the base formulation (Table 2, runs 1–30) plotted against the modified Kushner-Moore axis (Eq. (13)); plot is same data as Fig. 6A minus the bin blender data. Also shown are data and Eq. (13) fits at solid fraction of 0.80 (green) and 0.75 (blue), with 95% prediction intervals (dashed lines). (For interpretation of the references to colour in this figure legend, the reader is referred to the web version of this article.)

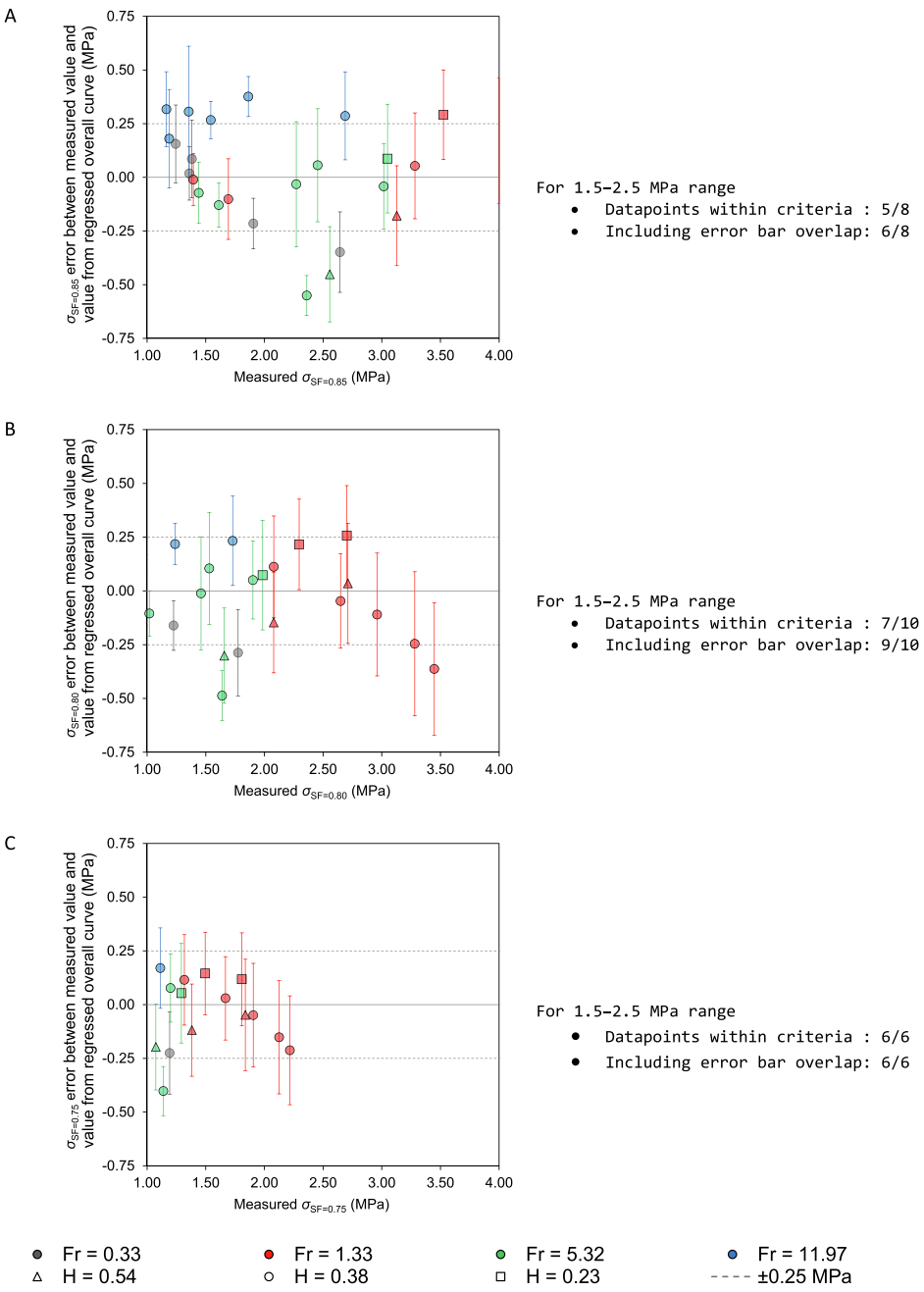

Fig. 8. Visualisation of errors between fitted curve of Fig. 6 and observed datapoints. Statistics to right of each plot are for key region of 1.5–2.5 MPa tensile strength at solid fraction 0.85–0.75 with target performance criteria of ± 0.25 MPa error (Nassar et al., 2021). A: solid fraction 0.85. B: solid fraction 0.80. C: solid fraction 0.75.

when the Froude number *Fr* is incorporated into the model equation, but only for situations where the Froude number was sufficiently high ($1 < Fr$). This is key as the mini-blender allows mixing at significantly higher speeds (and *Fr* values) than common batch blenders that are restricted to low speeds ($Fr < 0.4$) due to centrifugal forces preventing mixing (Brone et al., 1998). The results suggest that, aside from the number of revolutions experienced and mixing length scales which are important for both the mini-blender and common batch blenders, for the former it is the intensity of mixing captured by the Froude number as a surrogate which is important instead of the degree of fill or headspace (which is important for the latter). Although the present work chiefly explored blending time and contents mass as key dimensions and not blending length scales (which require similarly designed but smaller and / or larger systems), testing using alternative formulations showed the same common trend across mixing intensities when the modified equation incorporating Froude number was used, supporting the validity of the approach.

Results suggest that processing time in the mini-blender device can be reduced relative to tumble blending without affecting delivery of the desired lubrication extent and tensile strength of tablets made from the blended mixture, and that data from a few experiments at certain mixing intensities can be used to gain insight into the performance at other mixing intensities. The mini-blend technology allows easy access to a wide variety of lubrication extents depending on needs of process and the ability to drive process intensification in terms of lubrication cycle time when targeting a desired lubrication extent. The transferability of the present work has been tested with a bin blender, and literature has shown that bin blenders have mixing behaviour in common with other

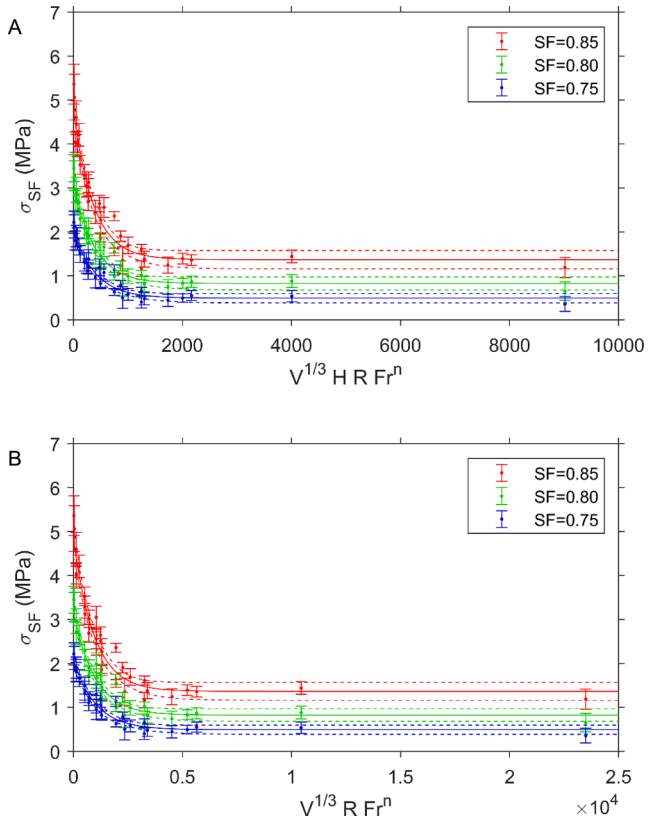

Fig. 9. Data and collapsed curves for the standard MCC (Pharmacel® 102)-heavy formulation using A: modified Kushner-Moore axis (Eq. (13)) and B: modified Kushner-Moore axis (Eq. (13)) with headspace fraction H omitted (*i.e.* $H = 1$). Most data points are with 3 kg of material (*i.e.* same H value) and their relative positions do not change when $H = 1$ (B).

Table 6
Regressed parameters for collapsed curves for 0.85, 0.80 and 0.75 solid fraction using the modified Kushner-Moore equation (Eq. (13)) with and without the use of headspace fraction H.

Solid fraction SF	Eq.	$\sigma_{SF,max}$ (MPa)	$\sigma_{SF,min}$ (MPa)	γ (dm^{-1})	RMSE
0.85	13	4.761 ± 0.395	1.369 ± 0.209	0.00272 ± 0.00071	0.685
	13 with $H = 1$	4.845 ± 0.406	1.366 ± 0.204	0.00106 ± 0.00027	0.675
0.80	13	3.134 ± 0.254	0.828 ± 0.149	0.00262 ± 0.00070	0.488
	13 with $H = 1$	3.183 ± 0.256	0.826 ± 0.143	0.00102 ± 0.00026	0.475
0.75	13	2.036 ± 0.178	0.494 ± 0.108	0.00248 ± 0.00070	0.372
	13 with $H = 1$	2.068 ± 0.178	0.494 ± 0.104	0.00097 ± 0.00026	0.362

batch blenders (Kushner and Moore, 2010). Results suggest that the proposed approach allows translation of lubrication extent between the different blending technologies such that experiments in batch blenders could be used to predict performance in the mini-blender, and vice versa, showing promise towards aiding process transfer between technologies and reducing the number of required experiments by using a common lubrication extent axis, improving material and time efficiency.

CRediT authorship contribution statement

Hikaru G. Jolliffe: Writing – review & editing, Writing – original draft, Investigation, Formal analysis, Data curation, Conceptualization.

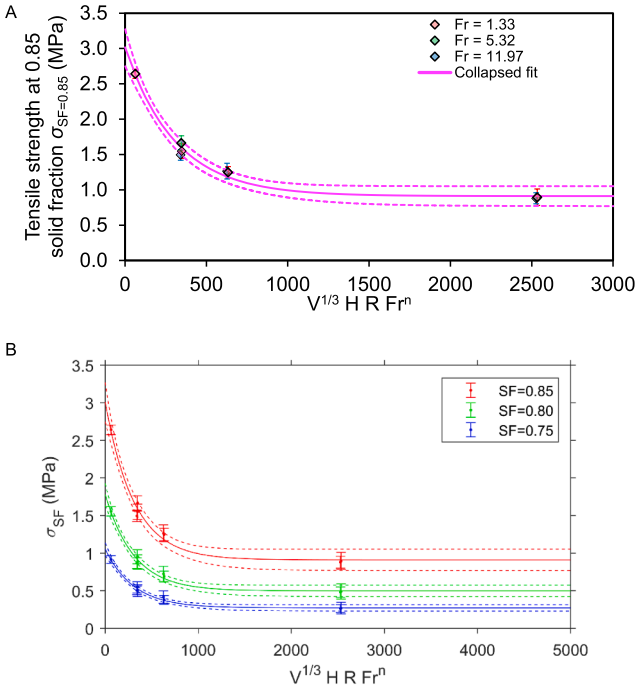

Fig. 10. Collapsed compaction data for the alternative high-lactose (SuperTab® 11SD) formulation (Table 2, runs 31– 38) plotted against the modified Kushner-Moore axis (Eq. (13)). A: solid fraction of 0.85, with separate colours for *Fr* of 1.33, 5.32, 11.97 correspond to 100, 200 and 300 RPM, respectively with fitted curve with prediction intervals. B: additionally plotting equivalent data at 0.80 and 0.75 solid fraction.

Table 7
Collapsed curve (Eq. (13)) regression parameters for high MCC (Pharmacel® 102) and high lactose (SuperTab® 11SD) formulations. Lubricant is 1.0 % Ligamed® MF-2 V for both formulations.

Formulation	$\sigma_{SF=0.85,max}$ (MPa)	$\sigma_{SF=0.85,min}$ (MPa)	γ (dm^{-1})	RMSE
66 % Pharmacel® 102, 33 % SuperTab® 11SD	4.761 ± 0.395	1.369 ± 0.209	0.00272 ± 0.00071	0.685
33 % Pharmacel® 102, 66 % SuperTab® 11SD	3.016 ± 0.263	0.911 ± 0.141	0.00324 ± 0.00081	0.265

Martin Prostredny: Methodology, Investigation, Formal analysis, Data curation. **Carlota Mendez Torrecillas:** Supervision, Methodology, Investigation, Data curation, Conceptualization. **Ecaterina Bordos:** Methodology, Investigation, Formal analysis, Data curation. **Collette Tierney:** Investigation, Formal analysis, Data curation. **Ebenezer Ojo:** Writing – original draft, Resources, Methodology, Investigation, Formal analysis, Data curation. **Richard Elkes:** Writing – review & editing, Supervision, Methodology, Investigation, Conceptualization. **Gavin Reynolds:** Supervision, Resources, Investigation, Conceptualization. **Yunfei Li Song:** Methodology, Investigation. **Bernhard Meir:** Writing – review & editing, Resources. **Sara Fathollahi:** Writing – review & editing, Resources. **John Robertson:** Writing – review & editing, Writing – original draft, Supervision, Project administration, Methodology, Investigation, Funding acquisition, Formal analysis, Data curation, Conceptualization.

Declaration of competing interest

The authors declare the following financial interests/personal relationships which may be considered as potential competing interests: Bernhard Meir reports a relationship with Gericke AG that includes: employment. Sara Fathollahi reports a relationship with DFE Pharma

GmbH & Co. KG that includes: employment. If there are other authors, they declare that they have no known competing financial interests or personal relationships that could have appeared to influence the work reported in this paper.

Data availability

Data will be made available on request.

Acknowledgements

This work has been funded by and conducted as part of the Medicines Manufacturing Innovation Centre (MMIC) project Grand Challenge 1 (CPI, n.d.); project ownership: Centre for Process Innovation (CPI). Funding has come from Innovate UK and Scottish Enterprise. Founding industry partners with significant financial and technical support are AstraZeneca and GSK (with special thanks to Gurjit Bajwa of GSK). The University of Strathclyde (via CMAC) is the founding academic partner. Project DFE Pharma have provided materials (special thanks to Bastiaan Dickhoff), partners Pfizer and have provided data and technical input to other project aspects, and project partners Gericke AG have provided technical equipment support and advice. Project partners Siemens and Applied Materials have provided key software and software engineering expertise to other aspects of MMIC GC1 work.

References

Brone, D., Alexander, A., Muzzio, F.J., 1998. Quantitative characterization of mixing of dry powders in V-blenders. AIChE J 44, 271–278. https://doi.org/10.1002/aic.690440206.

Busignies, V., Leclerc, B., Porion, P., Evesque, P., Couarraze, G., Tchoreloff, P., 2006. Compaction behaviour and new predictive approach to the compressibility of binary mixtures of pharmaceutical excipients. Eur. J. Pharm. Biopharm. 64, 66–74. https://doi.org/10.1016/j.ejpb.2006.03.004.

Busignies, V., Mazel, V., Diarra, H., Tchoreloff, P., 2012. Prediction of the compressibility of complex mixtures of pharmaceutical powders. Int. J. Pharm. 436, 862–868. https://doi.org/10.1016/j.ijpharm.2012.06.051.

CPI, n.d. Transforming tablet production - Grand Challenge 1 at the Medicines Manufacturing Innovation Centre [WWW Document]. URL https://www.uk-cpi.com/about/national-centres/grand-challenge-1 (accessed 11.24.23).

Dallinger, D., Kappe, C.O., 2017. Why flow means green – Evaluating the merits of continuous processing in the context of sustainability. Current Opinion in Green and Sustainable Chemistry, New Synthetic Methods 2017 (7), 6–12. https://doi.org/10.1016/j.cogsc.2017.06.003.

DiMasi, J.A., Grabowski, H.G., Hansen, R.W., 2016. Innovation in the pharmaceutical industry: New estimates of R&D costs. J. Health Econ. 47, 20–33. https://doi.org/10.1016/j.jhealeco.2016.01.012.

Duckworth, W., 1953. Discussion of Ryshkewitch Paper. J. Am. Ceram. Soc. 36.

Dwivedi, S.K., Oates, R.J., Mitchell, A.G., 1992. Estimation of elastic recovery, work of decompression and Young's modulus using a rotary tablet press. J Pharm Pharmacol 44, 459–466. https://doi.org/10.1111/j.2042-7158.1992.tb03647.x.

Fette, n.d. FE CPS - Continuous Processing System [WWW Document]. Fette Compacting. URL https://www.fette-compacting.com/en/products-technologies/continuous-manufacturing/fe-cps (accessed 4.5.24).

Galbraith, S.C., Park, S., Huang, Z., Liu, H., Meyer, R.F., Metzger, M., Flamm, M.H., Hurley, S., Yoon, S., 2020. Linking process variables to residence time distribution in a hybrid flowsheet model for continuous direct compression. Chem. Eng. Res. Des. 153, 85–95. https://doi.org/10.1016/j.cherd.2019.10.026.

García-Muñoz, S., Butterbaugh, A., Leavesley, I., Manley, L.F., Slade, D., Bermingham, S., 2018. A flowsheet model for the development of a continuous process for pharmaceutical tablets: An industrial perspective. AIChE J 64, 511–525. https://doi.org/10.1002/aic.15967.

GEA, 2016. Manufacturing medicines for today and the future [WWW Document]. URL https://www.gea.com/en/stories/continuous_manufacturing_technologies/ (accessed 4.5.24).

Gericke, 2023. Continuous Manufacturing [WWW Document]. https://www.gerickegroup.com/us/continuousmanufacturing (accessed 4.5.24).

Giannis, K., Schilde, C., Finke, J.H., Kwade, A., 2021. Modeling of high-density compaction of pharmaceutical tablets using multi-contact discrete element method. Pharmaceutics 13, 2194. https://doi.org/10.3390/pharmaceutics13122194.

Glatt, 2023. Continuous technologies pharma. URL https://www.glatt.com/products/continuous-technologies-pharma/ (accessed 4.5.24).

Gutmann, B., Kappe, C.O., 2015. Forbidden chemistries go flow in API synthesis - tks | publisher, event organiser, media agency. Chimica Oggi - Chemistry Today 33, 18–24.

Hosokawa Micron, n.d. Pharmaceutical Powder Mixing Systems [WWW Document]. URL https://www.hosokawa-micron-bv.com/solids-processing/pharmaceutical/pharma-powder-mixing-systems.html (accessed 4.5.24).

Ilić, I., Kása Jr., P., Dreu, R., Pintye-Hódi, K., Srčič, S., 2009. The compressibility and compactibility of different types of lactose. Drug Dev. Ind. Pharm. 35, 1271–1280. https://doi.org/10.1080/03639040902932945.

Janssen, P.H.M., Fathollahi, S., Bekaert, B., Vanderroost, D., Roelofs, T., Vanhoorne, V., Vervaet, C., Dickhoff, B.H.J., 2023. Impact of material properties and process parameters on tablet quality in a continuous direct compression line. Powder Technol. 424, 118520 https://doi.org/10.1016/j.powtec.2023.118520.

Jaspers, M., Roelofs, T.P., Lohrmann, A., Tegel, F., Maqsood, M.K., Song, Y.L., Meir, B., Elkes, R., Dickhoff, B.H.J., 2023. Process intensification using a semi-continuous mini-blender to support continuous direct compression processing. Powder Technol. 428, 118844 https://doi.org/10.1016/j.powtec.2023.118844.

Jolliffe, H.G., Papathanasiou, F., Prasad, E., Halbert, G., Robertson, J., Brown, C.J., Florence, A.J., 2019. Improving the prediction of multi-component tablet properties from pure component parameters, in: Kiss, A.A., Zondervan, E., Lakerveld, R., Özkan, L. (Eds.), Computer Aided Chemical Engineering, 29 European Symposium on Computer Aided Process Engineering. Elsevier, pp. 883–888. https://doi.org/10.1016/B978-0-12-818634-3.50148-X.

Karttunen, A.-P., Poms, J., Sacher, S., Sparén, A., Ruiz Samblás, C., Fransson, M., Martin De Juan, L., Remmelgas, J., Wikström, H., Hsiao, W.-K., Folestad, S., Korhonen, O., Abrahmsén-Alami, S., Tajarobi, P., 2020. Robustness of a continuous direct compression line against disturbances in feeding. Int. J. Pharm. 574, 118882 https://doi.org/10.1016/j.ijpharm.2019.118882.

Kushner, J., 2012. Incorporating Turbula mixers into a blending scale-up model for evaluating the effect of magnesium stearate on tablet tensile strength and bulk specific volume. Int. J. Pharm. 429, 1–11. https://doi.org/10.1016/j.ijpharm.2012.02.040.

Kushner, J., Moore, F., 2010. Scale-up model describing the impact of lubrication on tablet tensile strength. Int. J. Pharm. 399, 19–30. https://doi.org/10.1016/j.ijpharm.2010.07.033.

Kushner, J., Schlack, H., 2014. Commercial scale validation of a process scale-up model for lubricant blending of pharmaceutical powders. Int. J. Pharm. 475, 147–155. https://doi.org/10.1016/j.ijpharm.2014.08.036.

Lee, S.L., O'Connor, T.F., Yang, X., Cruz, C.N., Chatterjee, S., Madurawe, R.D., Moore, C.M.V., Yu, L.X., Woodcock, J., 2015. Modernizing pharmaceutical manufacturing: from batch to continuous production. J Pharm Innov 1–9. https://doi.org/10.1007/s12247-015-9215-8.

Lödige, 2023. Lödige as partner for the pharmaceutical industry [WWW Document]. URL https://www.loedige.de/en/industries/pharmaceuticals/ (accessed 4.5.24).

Lou, H., Kiang, Y.-H., Alvarez-Nunez, F., Li, W., Hageman, M.J., 2020. Modification of a scale-up model to improve prediction of the effect of lubrication on tablet tensile strength. Adv. Powder Technol. 31, 3080–3084. https://doi.org/10.1016/j.apt.2020.04.029.

Martin, N.L., Schomberg, A.K., Finke, J.H., Abraham, T.G., Kwade, A., Herrmann, C., 2021. Process modeling and simulation of tableting—an agent-based simulation methodology for direct compression. Pharmaceutics 13, 996. https://doi.org/10.3390/pharmaceutics13070996.

Moghtadernejad, S., Escotet-Espinoza, M.S., Oka, S., Singh, R., Liu, Z., Román-Ospino, A.D., Li, T., Razavi, S., Panikar, S., Scicolone, J., Callegari, G., Hausner, D., Muzzio, F., 2018. A Training on: continuous manufacturing (direct compaction) of solid dose pharmaceutical products. J Pharm Innov 13, 155–187. https://doi.org/10.1007/s12247-018-9313-5.

Nassar, J., Williams, B., Davies, C., Lief, K., Elkes, R., 2021. Lubrication empirical model to predict tensile strength of directly compressed powder blends. Int. J. Pharm. 592, 119980 https://doi.org/10.1016/j.ijpharm.2020.119980.

Palmer, J., Reynolds, G.K., Tahir, F., Yadav, I.K., Meehan, E., Holman, J., Bajwa, G., 2020. Mapping key process parameters to the performance of a continuous dry powder blender in a continuous direct compression system. Powder Technol. 362, 659–670. https://doi.org/10.1016/j.powtec.2019.12.028.

Pitt, K.G., Webber, R.J., Hill, K.A., Dey, D., Gamlen, M.J., 2015. Compression prediction accuracy from small scale compaction studies to production presses. Powder Technology, 6th International Workshop on Granulation: Granulation across the length scales 270, 490–493. https://doi.org/10.1016/j.powtec.2013.10.007.

Plumb, K., 2005. Continuous processing in the pharmaceutical industry - Changing the mind set. Chem. Eng. Res. Des. 83, 730–738. https://doi.org/10.1205/cherd.04359.

Ryshkewitch, E., 1953. Compression strength of porous sintered alumina and zirconia. J. Am. Ceram. Soc. 36, 65–68. https://doi.org/10.1111/j.1151-2916.1953.tb12837.x.

Schaber, S.D., Gerogiorgis, D.I., Ramachandran, R., Evans, J.M.B., Barton, P.I., Trout, B.L., 2011. Economic analysis of integrated continuous and batch pharmaceutical manufacturing: a case study. Ind. Eng. Chem. Res. 50, 10083–10092. https://doi.org/10.1021/ie2006752.

Vachon, M.G., Chulia, D., 1999. The use of energy indices in estimating powder compaction functionality of mixtures in pharmaceutical tableting. Int J Pharm 177, 183–200. https://doi.org/10.1016/s0378-5173(98)00347-0.

Wünsch, I., Finke, J.H., John, E., Juhnke, M., Kwade, A., 2019. A Mathematical approach to consider solid compressibility in the compression of pharmaceutical powders. Pharmaceutics 11, 121. https://doi.org/10.3390/pharmaceutics11030121.

Yoshida, J., Kim, H., Nagaki, A., 2011. Green and sustainable chemical synthesis using flow microreactors. ChemSusChem 4, 331–340. https://doi.org/10.1002/cssc.201000271.

Zhang, J., Wu, C.-Y., Pan, X., Wu, C., 2017. On identification of critical material attributes for compression behaviour of pharmaceutical diluent powders. Materials 10, 845. https://doi.org/10.3390/ma10070845.